



Contents lists available at ScienceDirect

Materials Today: Proceedings

journal homepage: www.elsevier.com/locate/matpr

Effect of zirconia/silica dopants on the thermally induced growth of sol gel synthesized cerium oxide nanoparticles

Thadathil S. Sreeremya

Department of Chemistry, Sree Narayana College, Kollam, India

ARTICLE INFO

Article history:

Received 4 May 2020

Accepted 9 May 2020

Available online xxxxx

Keywords:

Cerium

Zirconia

Silica

Thermal stability

Sol gel

Catalysis

ABSTRACT

Nanosized ceria, zirconia doped ceria and zirconia/silica co-doped catalytically important oxides possessing high specific surface area, and better thermal stability have been synthesized. The thermal and structural stability of the prepared oxides are strongly influenced by the synthetic methodology. In this study, aqueous sol-gel technique was adopted for preparation of pure and doped oxides. The prepared samples were further subjected to thermal treatments from 400 to 1300 °C in order to understand the nano-structural evolution and physicochemical characteristics of these complex oxide systems. Various physicochemical characterization techniques namely, thermal analysis (TG-DTA), X-ray diffraction (XRD), transmission electron microscopy (TEM), Photon Correlation Spectroscopy (PCS) and BET surface area (SA) were employed to investigate these oxide systems.

© 2020 Elsevier Ltd. All rights reserved.

Selection and peer-review under responsibility of the scientific committee of the International Conference on Energy and Environment.

1. Introduction

Within the category of oxides, ceria based materials have received much interest as catalysts and catalytic supports for use in diesel soot combustion, CO oxidation and VOCs abatement etc [1–3]. Catalytic applications of this interesting oxide stems from unique redox properties and the excellent oxygen storage capacity [4–7]. However ceria alone exhibits poor thermal stability and susceptible to sintering at high temperatures leading to catalyst deactivation [4].

Control of crystal growth (i.e., sintering) in inorganic nanostructured materials at elevated temperatures is highly important for applications in catalysis [8,9]. For example, exhaust stream catalysts are subject to temperatures upwards of 900 °C, which presents a thermodynamic driving force for crystallite growth. It has been reported that incorporation of Zr⁴⁺ into ceria could improve oxygen storage capacity, thermal stability [10] and also oxygen mobility. [1,11–15]. The incorporation of Zr⁴⁺ into CeO₂ can induce extrinsic defects associated with oxygen vacancy and also by the surface interactions with oxygen in the ceria-zirconia solid solutions [11]. Doping the third component such as transition metal oxide/rare earth oxide into the Ce_{1-x}Zr_xO₂ is confirmed to be effective in enhancing oxygen storage capacity and thermal stability [11]. Xiao et al. performed the first-principles molecular dynamics simulations to investigate the thermal stability of ceria-zirconia

solid solution surfaces. The calcining or ageing temperature at which specific surface area dramatically decreases was found to be 900–1000 K for pure ceria and 1073–1173 K for zirconium-ceria solid solutions with Zr/Ce ~1 [14]. Hybrid nanostructures of ceria-zirconia supported on silica was also found to be effective in improving thermal stability and activity of nano catalysts [15–18]. Ceria-Zirconia-Silica composites were utilised for CO reforming and explained the role of silica in improving thermal stability of ceria [11]. Various synthetic procedures adopted for preparing Ceria-zirconia, ceria-silica and metal impregnated Ceria-zirconia-silica includes precipitation method, sol gel method, evaporation induced self-assembly method, hydrothermal method, sonochemical method, reverse micelle etc [2,7,18,19]. Low cost, simplicity, purity of product, low temperature technique, better control of particle size, and high homogeneity of metal on the surface of the matrix makes sol gel method highly attractive [20,21].

Hence in the present work, sol-gel method was adopted for the synthesis of a series of silicon introduced Ce_{0.9}Zr_{0.1}O₂ (Si-CeZr) with variable Si/(Ce + Zr) molar ratios (0–0.2). The thermal stability of pure CeO₂ improved by Zr⁴⁺ incorporation, which was further improved to a great extent by the introduction of silica. Also, the prepared Si-CeZr nano catalysts may be suitable candidates for incorporation of metal nanoparticles to meet requirement in diverse industrial applications. Though synthesis of ceria-zirconia and ceria-zirconia-silica systems has been well documented, to

<https://doi.org/10.1016/j.matpr.2020.05.230>

2214-7853/© 2020 Elsevier Ltd. All rights reserved.

Selection and peer-review under responsibility of the scientific committee of the International Conference on Energy and Environment.

the best of our knowledge, no reports were available on the synthesis of ceria-zirconia-silica nanocomposites entirely by aqueous sol gel route.

2. Experimental

2.1. Synthesis of CeZrSi-x catalysts by aqueous sol-gel technique

Zr and Si co-doped ceria represented as CeZrSi-x where x refers to molar ratio of Si to Ce + Zr, ranging from 0 to 0.2. In a typical experiment, required amount of cerium nitrate hexahydrate ($\text{Ce}(\text{NO}_3)_3 \cdot 6\text{H}_2\text{O}$) was dissolved in 250 mL of distilled water to make a 0.2 M solution and was precipitated by slow addition of ammonium hydroxide solution under constant stirring at room temperature, until the pH was 7.7. The precipitate was filtered, washed and was peptised using 2 M HNO_3 till pH \sim 2. For the synthesis of Zr^{4+} doped ceria sol, mixed precursors of $\text{Ce}(\text{NO}_3)_3 \cdot 6\text{H}_2\text{O}$, and $\text{ZrOCl}_2 \cdot 8\text{H}_2\text{O}$ were used. Further 4, 8, 10, 15 and 20 mol% Zr^{4+} doped ceria sol was prepared by the same procedure. When the mol% of Zr^{4+} was increased beyond 10%, a deterioration in the stability of the sol was observed after few days. Hence 10 mol% Zr^{4+} doped ceria sol (will be named as CeZr now onwards) was selected for all further studies. A silica sol was prepared from tetraethoxysilane (Aldrich Chemicals, USA) by controlled hydrolysis using 0.001 M HCl (Ranbaxy Fine Chemicals, India) in isopropanol (Ranbaxy Fine Chemicals, India) medium. Tetraethoxysilane, isopropanol and water were mixed at a molar ratio of 1:4:16 [22] and stirred for 1 h to prepare the silica sol. To the stable CeZr sol, silica sol was added under strong mechanical stirring in such a way to prepare Si-CeZr in which the ratio of Si/(Ce + Zr) was varied from 0 to 0.2. The sol was dried and the dried powder was then calcined at 400, 900 and 1300 °C for one hour.

2.2. Characterisation of the catalyst

The crystalline phase composition of the solid products were determined from the powder X-ray diffraction (XRD) patterns using a Philips X'PERT PRO diffractometer with Ni-filtered $\text{Cu K}\alpha_1$ radiation ($\lambda = 1.5406 \text{ \AA}$) in the 2θ range 20–100° at a scanning rate of 2° min^{-1} with a step size 0.04° . The morphology, average size of the CeO_2 crystals and crystal structure were determined by high resolution transmission electron microscopy (HR-TEM) using a FEI Tecnai 30 G² S-Twin microscope operated at 300 kV and equipped with a Gatan CCD camera. The nanocatalysts were also examined using scanning electron microscope (JEOL-JSM-5600LV, Japan) operated at 15 kV. Size measurements for the colloidal cerium oxide NPs in suspensions were performed at 25 °C by photon correlation spectroscopy (PCS) on a Zetasizer 3000 HSA, Malvern Instruments, Worcestershire, UK using a 60 mW He-Ne laser operating at a wavelength of 633 nm with General Purpose algorithm with Dispersion Technology Software (v. 1.61) at 90° detection angle. The surface area measurements were carried out by nitrogen adsorption using Micromeritics Gemini 2375 surface area analyzer, after degassing the sample at 200 °C for 2 h.

3. Results and discussion

3.1. X-ray diffraction analysis

The recorded XRD patterns for all the nanocatalysts synthesised through sol-gel technique, are presented in Fig. 1. The XRD profiles for all the nanopowders match with the face-centred cubic [space group: $Fm\bar{3}m$ (2 2 5)] of crystalline CeO_2 (JCPDS Card No. 34-394) with fluorite-type structure in which each metal cation is surrounded by eight oxygen atoms [23–25].

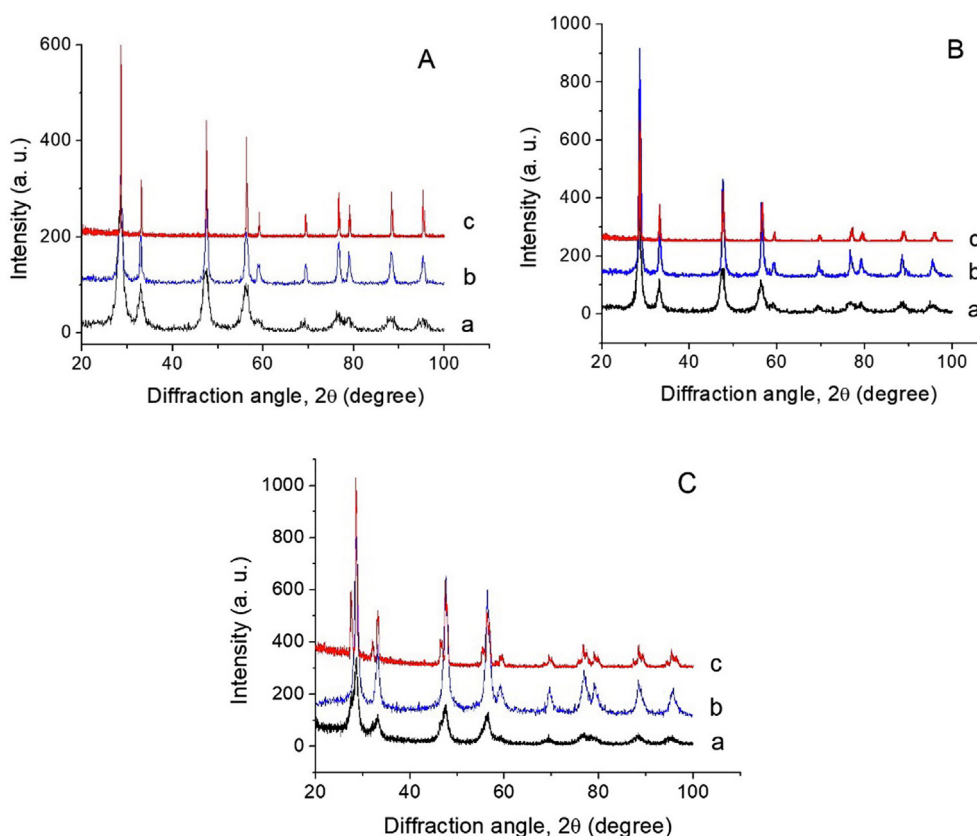


Fig. 1. XRD patterns of (A) Ce (B) CeZr (C) CeZrSi-0.2 calcined at (a) 400 °C (b) 900 °C, and (c) 1300 °C.

The crystallite size of samples, D_{XRD} was estimated by applying full-width-half-maximum (FWHM) of characteristic peak (1 1 1) to the Scherrer formula and lattice parameter was calculated which are presented in Table 1.

The general trend of growth of crystals with increase in calcination temperature was observed for all the samples as evidenced by the narrowing of XRD peaks as we move from 400 to 1300 °C calcined samples. The beneficial property of Zr^{4+} and Si^{4+} in mitigating the extent of grain growth at high temperatures [9,11,12,26] is clearly observed by the broadening of XRD peaks of CeZr and CeZrSi-x samples which indicate smaller crystals and poor crystallinity for the Zr^{4+} and Si^{4+} co-doped samples. Pure Ce has grown from 9.4 nm to 43 nm (~5 times crystal growth) on increasing the calcination temperature from 400 to 1300 °C whereas it is only ~4 times in the case of CeZr and 3 times for CeZrSi-0.2. The fluorite structure of ceria has been observed for all the Zr^{4+} doped and $\text{Zr}^{4+}/\text{Si}^{4+}$ co-doped samples, suggesting that ZrO_2 was incorporated into the CeO_2 lattice to form a solid solution while maintaining the fluorite structure [12]. From the figure it can be observed that the diffraction peaks were shifted to higher two theta angles when Zr^{4+} and $\text{Zr}^{4+}/\text{Si}^{4+}$ is incorporated into CeO_2 . This observation indicates a shrinkage of the lattice due to the replacement of Ce^{+4} with much smaller Zr^{+4} ions in the case of CeZr and $\text{Zr}^{4+}/\text{Si}^{4+}$ in CeZrSi-0.2, this coincides with the fact that the cation radius of Zr^{+4} (0.84 Å) and Si^{4+} (0.42 Å) is less than that of Ce^{+4} (1.09 Å) [27,28]. Mixing zirconia/silica with ceria is reported to reduce the lattice constant and produce the atomic-level pressure at the smaller

tetrahedral sites, making them even more difficult to reach for the interstitial oxygen ions than in pure ceria, thus enhancing the stability of oxygen defects against thermal aging in ceria-zirconia.

3.2. Size analysis by photon correlation spectroscopy

The size measurement data from static light scattering for pure and doped ceria in aqueous suspensions are given in Fig. 2. Z-average diameters are the mean hydrodynamic diameter based upon the intensity of scattered light estimated from the analysis of the correlograms. In pure and doped samples, the polydispersity index (PDI) value was between 0.3 and 0.5, indicating agglomeration of the fine sized particles in aqueous medium. The PDI estimates the width of the distribution. PDI value above 0.3 does not indicate a monodisperse suspension [29]. The particle size measurements also followed the same trend as in the case of XRD. The particle size for pure ceria sample increased from 65 to 129 nm on increasing the calcination temperature from 400 to 1300 °C.

The particle size for all the samples followed the order $\text{Ce} > \text{CeZr} > \text{CeZrSi-0.2}$ at all calcination temperatures, further confirming the role of Zr^{4+} and Si^{4+} in controlling the growth of nanoparticles with respect to calcination temperature.

3.3. BET surface area analysis

The N_2 BET surface areas of various samples synthesized in this study and calcined at 400–1300 °C are presented in table 2 which supports the XRD and PCS data. The incorporation of Zr^{4+} into the CeO_2 arrested crystal growth resulting in an increase of specific surface area from 35.2 to 79.1 $\text{m}^2 \text{g}^{-1}$. Further incorporation of Si into the CeZr host structure added to this effect and surface area steadily augmented with increasing silica content and reached a maximum of 123.8 $\text{m}^2 \text{g}^{-1}$ by 20 mol% Si^{4+} incorporation. Sintering of the nanocrystalline network occurred during the thermal treatments decreasing the surface area for all the samples. The cerium

Table 1
Crystal size and lattice constants of ceria samples calcined at different temperatures.

SAMPLE	Crystal size (nm)/Lattice parameter (Å)		
	400 °C	900 °C	1300 °C
Ce	9.4/5.412	18.2/5.408	43/5.406
CeZr	7.6/5.394	13.8/5.382	28.5/5.355
CeZrSi-0.2	6.7/5.387	9.1/5.376	21/5.361

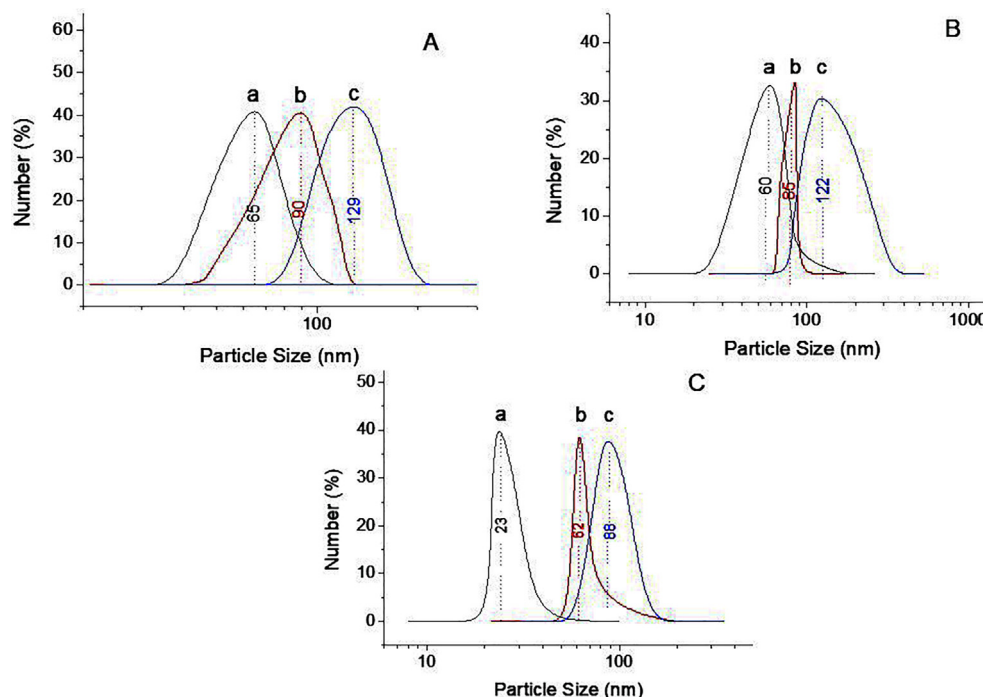


Fig. 2. Particle size variation of (A) Ce (B) CeZr (C) CeZrSi-0.2 at (a) 400 °C (b) 900 °C, and (c) 1300 °C.

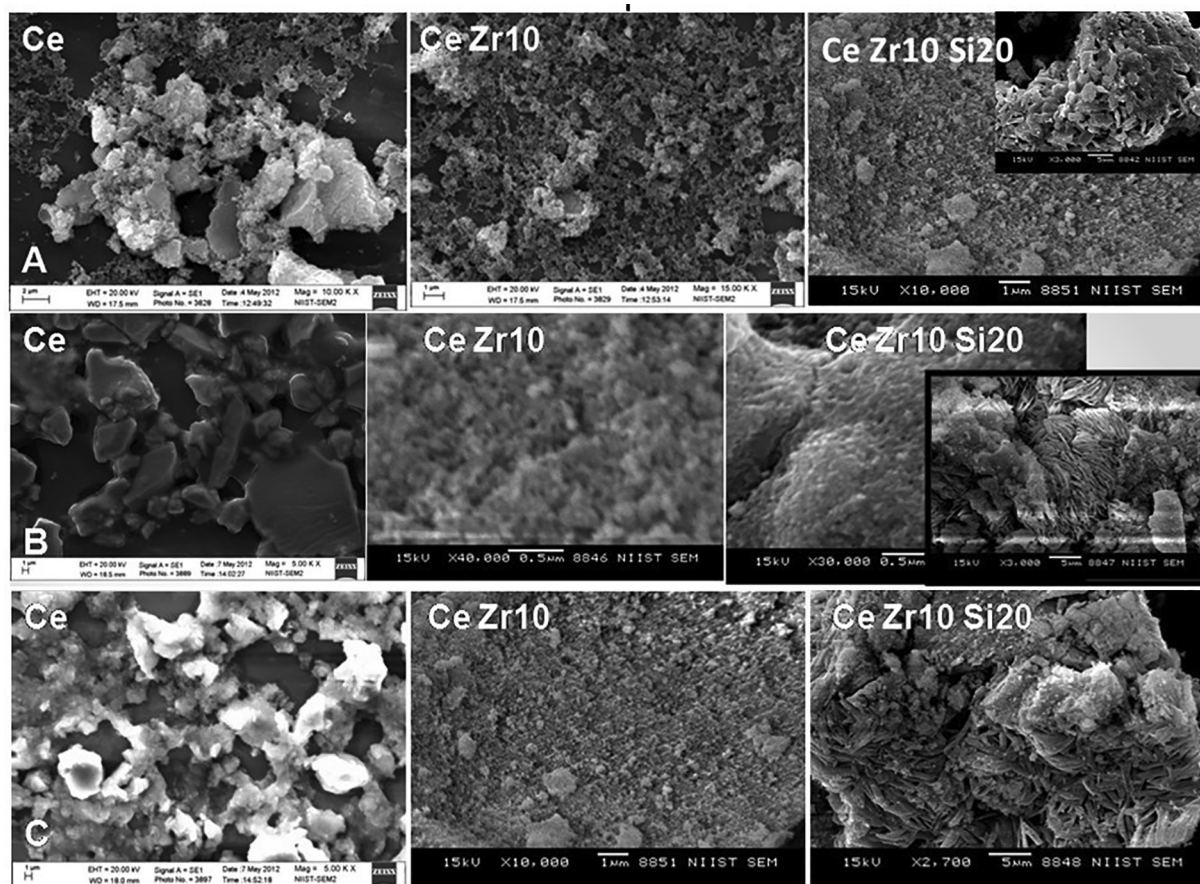


Fig. 3. SEM images of samples calcined at A) 400 °C, B) 900 °C, and C) 1300 °C.

Table 2
Surface area analysis of ceria samples calcined at different temperatures.

Sample	Surface Area (m ² /g)			% Reduction in SA	
	400 °C	900 °C	1300 °C	900 °C	1300 °C
Ce	35.2	1.98	-ve adsorption	94	100
CeZr	79.1	30.7	-ve adsorption	61	100
CeZrSi-0.05	84.9	41.4	-ve adsorption	51.2	100
CeZrSi-0.1	91.5	45.3	-ve adsorption	50.5	100
CeZrSi-0.15	104.4	51.61	0.151	50.6	99.8
CeZrSi-0.2	123.8	67.4	0.431	45.1	99

only samples exhibited by far the greatest decrement in specific surface area e.g., 94% decrease to 2 m² g⁻¹ at 900 °C and ~ 100% decrease at 1300 °C. Conversely, CeZr and CeZrSi-0.2 maintained specific surface area of 30.7 m² g⁻¹ and 67.4 m² g⁻¹ respectively at 900 °C.

Detailed pore analysis of all the samples is required which is not done in the present study.

3.4. Electron microscopic studies

3.4.1. SEM analysis

The morphology and microstructure of the ceria (CeO₂) product was investigated using SEM. The SEM image of the ceria product after thermal treatments (400–1300 °C) is shown in Fig. 3. Please note that all images are not of the same magnification and are intended to show only the porosity of the samples.

It is clear from the SEM images that Zr and Zr/Si doped ceria is more porous than pure ceria and the pores have become more or

less uniform in the doped and co-doped samples. Presence of elongated structures can be seen in CeZrSi samples which was found to increase with the calcination temperature, in support of Fig. 4C.

3.4.2. TEM analysis

The bright-field high resolution transmission electron microscopy images of pure and doped CeO₂ crystals prepared by sol gel route are shown in Fig. 4. Morphology of the pure and doped nanocrystals appear almost irregular at 400 °C (Fig. 4A). Less crystallinity was observed for CeZr and CeZrSi-0.2 in agreement with the broadened peaks in Fig. 1B. A careful morphological analysis of the CeZr and CeZrSi heat treated at 900 °C reveals the presence of nanopolyhedra (i.e. truncated octahedral) with sizes of about 20–30 nm and 10–20 nm respectively. In addition to polyhedral shapes, a few elongated structures were also observed in CeZr and CeZrSi in Fig. 4 B and C. This can be attributed to the fact that crystal planes of same type tend to align with each other to minimize the interface strain, [2] forming a coherent interface. The

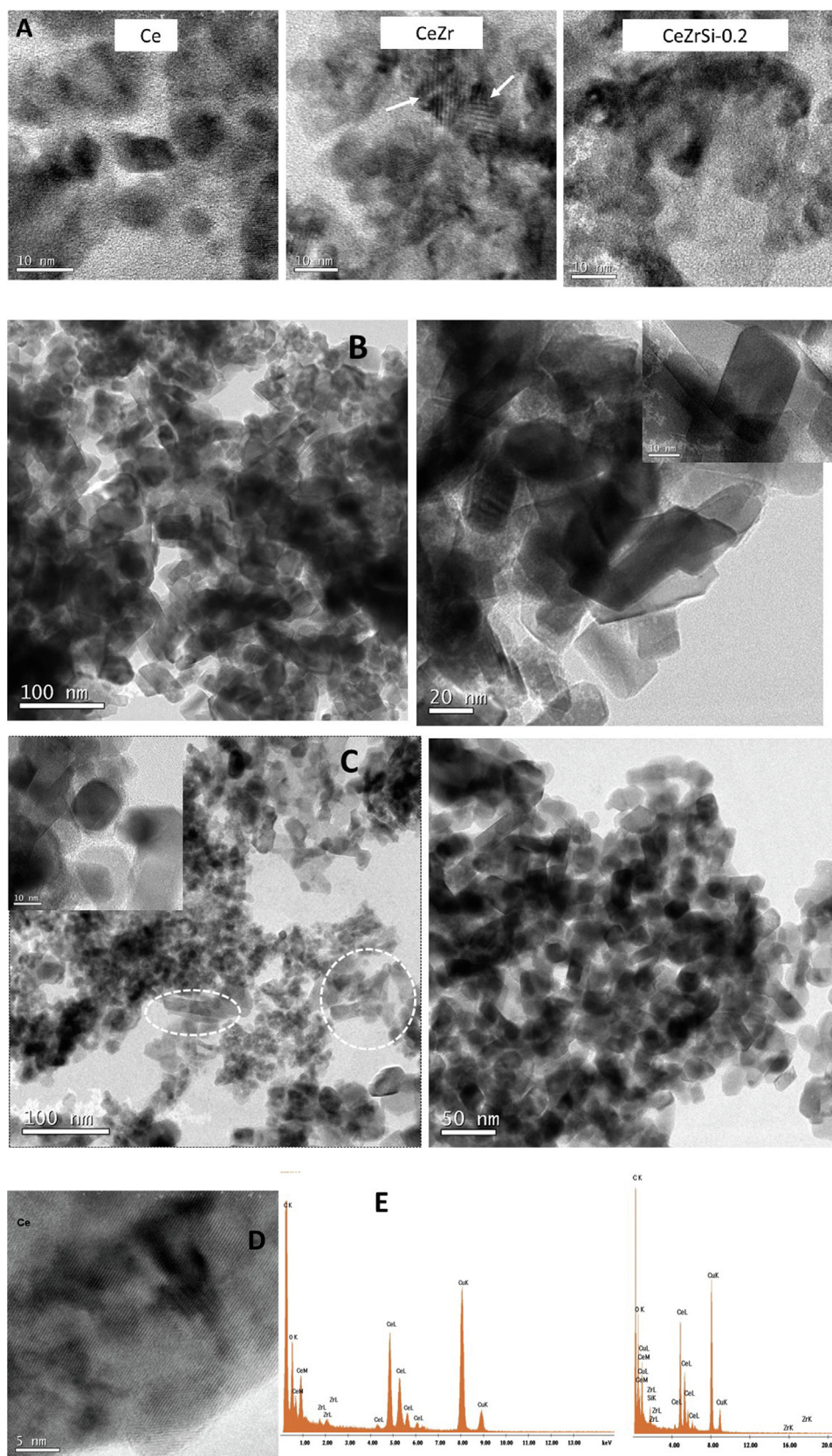


Fig. 4. TEM images of undoped and doped catalyst at A) 400C B) CeZr at 900C C) CeZrSi-0.2 at 900C D) Ce at 1300C E) EDX characterisation for CeZr and CeZrSi-0.2.

structural defects (e.g. terraces, ledges and kinks) formed by substitution of Ce^{4+} cations with Zr^{4+} are indicated using arrow heads in Fig. 4A.

Structural defects can favour the mobility of charged species, such as electrons or oxygen anions in the solid catalyst and are considered to be essential for generating catalytic active species.

Large particles of size over 50 nm formed during the calcination of pure CeO₂ at 1300 °C (Fig. 4D) which may be the reason of showing -ve adsorption of nitrogen at liquid nitrogen temperature. Also, the EDS pattern shown in Fig. 4E reveals the presence of Ce, Zr, O elements in CeZr and Ce, Zr, Si, O elements in CeZrSi.

3.5. Role of zirconia and silica

Silica may be serving as a glue linking the ceria nanoparticles to inhibit the growth of crystals which results in improvement in thermal stability of CeZrSi-x, [11]. Presence of silica also improve surface area, one of the pre requisites for a catalyst. Ceria is known to exhibit a dramatic drop in the concentrations of vacancies and interstitial ions on heat treatment. The substitution of Ce⁴⁺ cations with Zr⁴⁺ promotes the formation of structural defects (e.g. terraces, ledges and kinks) on the catalyst surface, which was evident from TEM images. Structural defects can favour the mobility of charged species, such as electrons or oxygen anions in the solid catalyst and are considered to be essential for generating catalytic active species. Zirconia can prevent loss of surface area at high temperature by inhibiting surface diffusion and can also stabilise oxygen defective structure of ceria.

4. Conclusions

The present investigation included the effect of doping in cerium oxide with different cations on the resistance to growth of ceria particles during annealing for a possible application in the area of high temperature catalysis. Using sol gel technique a series of catalytically important Zr⁴⁺ and Zr⁴⁺/Si⁴⁺ co-doped nanosized cerium oxides possessing high specific surface area and better thermal stability have been synthesized. The particle size for all the samples followed the order Ce > CeZr > CeZrSi-0.2 at all calcination temperatures confirming the role of Zr⁴⁺ and Si⁴⁺ in controlling the growth of nanoparticles with respect to calcination temperature. Presence of silica and zirconia additives were reported to improve the dispersity of metal nanoparticles and hence the thermally stable CeZrSi prepared via simple sol gel technique can be utilised for the development of efficient metal incorporated nanocatalysts.

CRedit authorship contribution statement

Thadathil S. Sreeremya: Conceptualization, Methodology, Writing - original draft.

Declaration of Competing Interest

The authors declare that they have no known competing financial interests or personal relationships that could have appeared to influence the work reported in this paper.

Acknowledgements

The authors are grateful to the Director, National Institute for Interdisciplinary Science & Technology (NIIST), CSIR for providing the necessary facilities for the work. Author acknowledges CSIR for the CSIR-UGC SRF fellowship. Authors thank Head, S. N. College, Kollam, Kerala for all the lab facilities.

References

- [1] M. Piumetti, S. Bensaïd, N. Russo, D. Fino, *Appl. Catal. B: Environ.* 180 (2016) 271–282.
- [2] T.S. Sreeremya, A. Krishnan, K.C. Remani, K.R. Patil, F. Dermot, Brougham, S. Ghosh, *ACS Appl. Mater. Interfaces* 7 (16) (2015) 8545–8555.
- [3] A. Trovarelli, J. Llorca, *ACS Catal.* 7 (2017) 4716–4735.
- [4] C.L. Li, X. Gu, Y.Q. Wang, Y.J. Wang, Y.G. Wang, X.H. Liu, G.Z. Lu, *J. Rare Earths* 27 (2009) 211–215.
- [5] A. Trovarelli, M. Boaro, E. Rocchini, C. de Leitenburg, G. Dolcetti, *J. Alloys Compd.* 323 (2001) 584–591.
- [6] H. Zou, Y.S. Lin, N. Rane, T. He, *Ind. Eng. Chem. Res.* 43 (2004) 3019–3025.
- [7] H.X. Mai, L.D. Sun, Y.W. Zhang, R. Si, W. Feng, H.P. Zhang, H.C. Liu, C.H. Yan, *J. Phys. Chem. B* 109 (2005) 24380–24385.
- [8] D. Devaiah, L.H. Reddy, S.E. Park, B.M. Reddy, *Catal. Rev.* 60 (2) (2018) 177–277.
- [9] N.C. Strandwitz, S. Shaner, G.D. Stucky, *J. Mater. Chem.* 21 (2011) 10672–10675.
- [10] V. Raju, S. Jaenicke, G.K. Chuah, *Appl. Catal. B: Environ.* 91 (2009) 92–100.
- [11] X. Xiang, H. Zhao, J. Yang, J. Zhao, L. Yan, H. Song, L. Chou, *Appl. Catalysis A: Gen.* 520 (2016) 140–150.
- [12] D. Hari Prasad, J.-H. Lee, H.-W. Lee, B.-K. Kim, J.-S. Park, *J. Ceramic. Process. Res.* 10 (2009) 748.
- [13] R. Wang, Peter A. Crozier, Sharma R., James B. Adams, *J. Phys. Chem. B*, 2006, 110, 18278–18285.
- [14] G. Zhou, Wen-Tong Geng, W. Xiaoa, L. Suna, J. Wang, L. Wang, *Appl. Surf. Sci.* 507 (2020) 144942.
- [15] P. Munusamy, S. Sanghavi, T. Varga, T.S. Pillai, *RSC Adv.* 4 (2014) 8421.
- [16] I. Sulym, D. Sternik, L. Oleksenko, L. Lutsenko, M. Borysenko, *Surfaces Interfaces* 5 (2016) 8–14.
- [17] N.N. Gavrilova, V.V. Nazarov, *Inorg. Mater.* 54 (2018) 831–839.
- [18] H. Wang, J.J. Zhu, J.M. Zhu, X.H. Liao, S. Xu, T. Ding, H.Y. Chen, *Phys. Chem. Chem. Phys.* 4 (2002) 3794–3799.
- [19] T. Masui, K. Fujiwara, K. Machida, G. Adachi, T. Sakata, H. Mori, *Chem. Mater.* 9 (1997) 2197–2204.
- [20] N. Rane, H. Zou, G. Buelna, Jerry Y.S. Lin, *J. Membr. Sci.* 256 (2005) 89–97.
- [21] J.J. Gulicovski, S.K. Milonji, K. Mészáros Szécsényi, *Mater Manuf. Process.*, 2009, 24, 1080–1085.
- [22] Ranga Rao, B.G. Mishra, *Bull. Catal. Soc. India* 2 (2003) 122–134.
- [23] S. Kar, C. Patel, S. Santra, *J. Phys. Chem. C* 113 (2009) 4862–4867.
- [24] T. Masui, K. Machida, T. Sakata, H. Mori, G. Adachi, *J. Alloys and Compd.* 256 (1997) 97–101.
- [25] T. Garcia, B. Solsona, S.H. Taylor, *Catalysis Lett.* 105 (2005) 183–189.
- [26] Ruigang Wang, Peter A. Crozier, Renu Sharma, *J. Mater. Chem.* 20 (2010) 7497–7505.
- [27] N.D. Petkovich, S.G. Rudisill, L.J. Venstrom, D.B. Boman, Jane H. Davidson, Andreas Stein, *J. Phys. Chem. C* 115 (2011) 21022–21033.
- [28] B.M. Reddy, A. Khan, *Catalysis Surveys Asia* 9 (2005) 155–171.
- [29] J.K. Stolarczyk, S. Ghosh, D.F. Brougham, *Angew. Chem., Int. Ed.* 48 (2009) 175–178.